

Fast Restoration Algorithm for Hybrid HVDC Grids

M.DU
University of Waterloo
Canada

S.P.AZAD
University of Waterloo
Canada

SUMMARY

High voltage direct current (HVDC) systems based on modular multi-level converters (MMCs) can be utilized for large integration of distributed renewable energy resources into power grids and to transfer bulk energy over long distances economically. In modern power systems, point-to-point HVDC transmission lines can be expanded to form multi-terminal HVDC systems or even HVDC grids. Since in future HVDC grids, different types of MMCs, such as half-bridge MMCs (HB-MMCs) or full-bridge MMCs (FB-MMCs), may be used and operate simultaneously, the different fault-response characteristics of MMCs may increase the complexity of the protection scheme including the restoration process. This paper proposes an algorithm for the restoration of various types of HVDC grids, which may even contain different types of converters with and without fault blocking capability. Three types of four-terminal HVDC grids are tested in this paper, namely, a grid which contains only FB-MMCs, only HB-MMCs, and a combination of FB-MMCs and HB-MMCs. Simulation results show that the proposed restoration algorithm can restore different types of HVDC grids in less than 40 ms with low voltage oscillations and limited inrush currents.

KEYWORDS

High voltage direct current (HVDC) grid, Restoration, Full-bridge modular multi-level converter (FB-MMC), Half-bridge MMC (HB-MMC)

1 INTRODUCTION

High voltage direct current (HVDC) grids based on modular multi-level converters (MMCs) have great advantages over high voltage alternating current (AC) transmission lines for transferring bulk electric power over long distances and connecting asynchronous power systems [1, 2]. As a promising medium to future integrates the distributed renewable energy resources into the power grid, several MMC-HVDC projects are implemented in North America, China, and Europe [3–5]. With the increasing demand for renewable resources and the development of HVDC grids, existing point-to-point HVDC transmission lines may be expanded to multi-terminal HVDC grids (MTDC) in modern power systems. In future power grids, various types of MMCs with different fault response characteristics may operate simultaneously.

Various methods for protection of MMCs with different fault-response characteristics are proposed in [2, 5–11]. When a half-bridge MMC (HB-MMC) is blocked, it cannot interrupt the fault current due to the freewheeling-diodes. An AC circuit breaker (ACCB) inserted between the HB-MMC and the AC grid can be used to clear the fault. Since mechanical ACCBs must wait for the current zero-crossing point to open, ACCBs normally take a few cycles (tens of ms) to operate. Unlike HB-MMCs, full-bridge MMCs (FB-MMCs) and clamp double MMCs (CD-MMCs) can drive the fault current to zero after they are blocked. Thus, in an HVDC grid with only FB- or CD-MMCs, faults can be cleared in a few ms by blocking all MMCs [2]. Since sub-modules (SMs) of FB- and CD-MMCs can insert both positive and negative voltages into the fault current path, FB- and CD-MMCs can also clear the fault without being blocked [6]. However, FB- and CD-MMCs require more semiconductor devices compared to HB-MMCs, which will increase the converter cost and conduction losses. An alternative approach to protect HVDC grids is to use DC circuit breakers (DCCBs). By isolating the faulty part in a few ms, DCCBs can maintain power transmission in the healthy part of the grid [7]. For HVDC grids with DCCBs, selective fault detection algorithms are proposed to detect and identify the fault in several ms [5, 8, 9]. Fault current limiters (FCLs) are also used to increase the performance of DCCBs [7, 10]. Although protection schemes based on DCCBs are selective and reliable, DCCBs are expensive and are not yet used in real-world HVDC grids [11].

After the fault clearance, the HVDC grid should be restored. In [2], an algorithm is proposed to restore a four-terminal FB-MMC-based HVDC grid under a permanent fault. In [2], even though FB-MMCs can interrupt the fault current, an ACCB is inserted between each FB-MMC and the AC grid, and after the grid is discharged and the faulty section is isolated with disconnectors, the restoration begins. In the restoration process of [2], ACCBs are first closed, and then the voltage-controlling FB-MMC is de-blocked. The other three power-controlling FB-MMCs are de-blocked when the DC voltage at the respective terminals is above 90% of the nominal value for more than 20 ms. Right after de-blocking of the power-controlling MMCs for almost 1 s, the power set-points are set to zero to limit the inrush currents. Another algorithm is proposed in [6] to restore an HVDC grid under a temporary fault without blocking the MMCs. However, this algorithm cannot be used in HVDC grids with HB-MMCs because HB-SMs cannot insert negative voltages into the fault current path, and consequently cannot interrupt the fault current. To protect the insulated-gate bipolar transistor (IGBT) switches in an HB-MMC during faults, the converter SMs should be necessarily blocked.

The few proposed algorithms for the restoration of HVDC grids, only consider one type of converter technology, i.e., MMCs with or without fault blocking capability. This paper proposes an algorithm for restoration of HVDC grids with any combination of FB-MMCs and HB-MMCs. Therefore, the proposed restoration algorithm of this paper can be applied to hybrid HVDC grids as well as HVDC systems with either FB-MMCs or HB-MMCs.

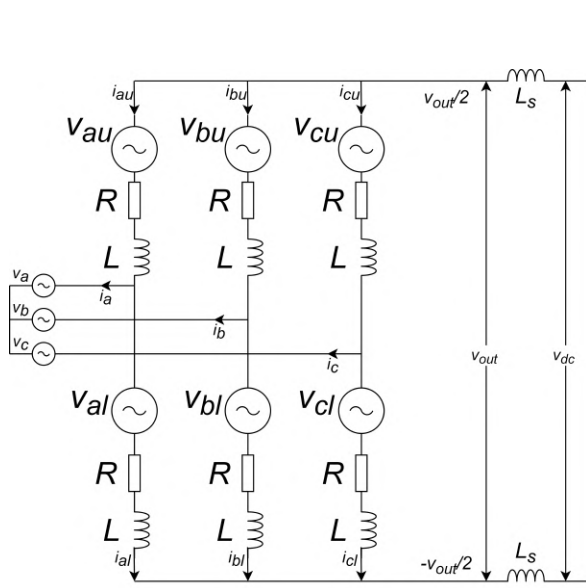


Figure 1: The simple schematic of an MMC

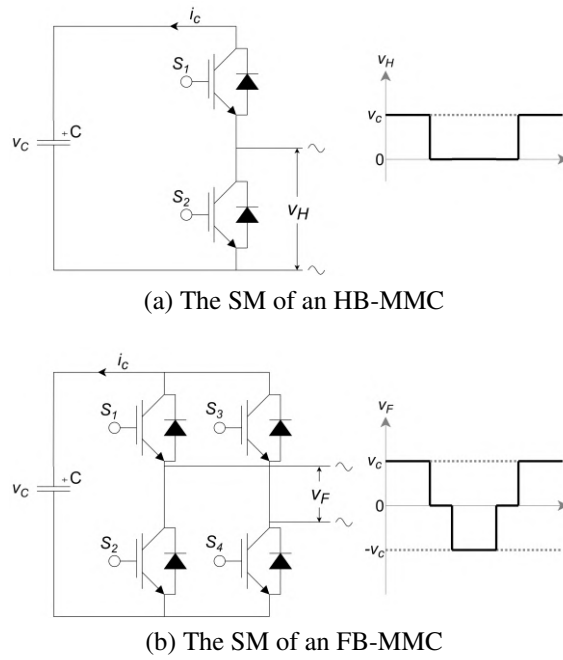


Figure 2: SMs of two types of MMCs.

In this paper, restoration of FB-MMCs and HB-MMCs are studied in Section 2. The test grids used for the studies of this paper are introduced in Section 3. The proposed restoration algorithm for hybrid HVDC grids is discussed in Section 4. Simulation results are provided in Section 5 to evaluate the performance of the proposed restoration algorithm. Finally, conclusions are given in Section 6.

2 MODELING OF FB- AND HB-MMCs

As shown in Figure 1, an MMC consists of a large number of SMs connected in series in each arm. Two types of MMCs, HB-MMCs and FB-MMCs are studied in this paper. An FB-MMC can interrupt the fault current while an HB-MMC cannot [10]. An FB-SM can generate a bipolar output voltage while the HB-SM can only generate a monopolar output voltage as shown in Figure 2.

In Figure 1, the nominal DC grid voltage is V_{dc} , and voltages of the positive and negative poles are $\frac{V_{dc}}{2}$ and $-\frac{V_{dc}}{2}$, respectively. The AC grid phase voltage is $v_x = \frac{\sqrt{2}}{2} V_m \sin(\omega t + \phi_x)$, where $x \in \{a, b, c\}$ denotes the phase and V_m is the peak AC phase voltage. Each leg of the MMC is divided into an upper arm (u) and a lower arm (l). By controlling the number of SMs inserted into each arm, the upper arm voltage (v_{xu}) and the lower arm voltage (v_{xl}) in leg x is controlled. During the normal operation, the set-points for the arm voltages are determined by (1), where v_{out}^* is the set-point of the MMC DC terminal voltage.

$$\begin{cases} v_{xu}^* = \frac{v_{out}^*}{2} - v_x - L \frac{di_{xu}}{dt} - Ri_{xu}, \\ v_{xl}^* = \frac{v_{out}^*}{2} + v_x - L \frac{di_{xl}}{dt} - Ri_{xl}. \end{cases} \quad (1)$$

When a converter is de-blocked at t_{db} during the restoration process, the MMC DC terminal voltage v_{out} should be close to the grid DC voltage v_{dc} ; otherwise, the voltage difference between the DC grid and the MMC terminal will lead to a large inrush current and voltage oscillations. Therefore, to ensure a smooth restoration, v_{out}^* should be selected such that the MMC generates a terminal voltage v_{out} that is close to the grid voltage. An FB-MMC can be controlled

such that the terminal voltage $v_{out,FB}$ reaches any voltage set-points $v_{out,FB}^*$ as FB-SMs can insert both positive and negative voltages in the converter arms. So in an FB-MMC $v_{out,FB}^* = v_{dc}$ can be selected to generate a terminal voltage $v_{out,FB}$, which is the same as the HVDC grid voltage during the restoration process. On the contrary, for an HB-MMC the converter DC terminal voltage $v_{out,HB}$ may not be able to track all set-point voltages $v_{out,HB}^*$ as HB-SMs can only generate positive or zero voltages. For example, if $v_{out,HB}^* = 0$, one of the arm-voltage set-points v_{xu}^* or v_{xl}^* becomes negative according to (1). Since HB-SMs cannot generate negative voltages, $v_{out,HB}$ cannot follow the set-point $v_{out,HB}^*$ and will not become zero. To better understand this, the relationship between $v_{out,HB}$ and $v_{out,HB}^*$ in an HB-MMC is determined:

$$v_{out,HB} = (v_{xu} + v_{xl}) + R(i_{xu} + i_{xl}) + L \frac{d(i_{xu} + i_{xl})}{dt}. \quad (2)$$

Assuming $\sum_x^{a,b,c} i_{xu} = \sum_x^{a,b,c} i_{xl} = 0$,

$$3v_{out,HB} - \sum_x^{a,b,c} (v_{xu} + v_{xl}) = R \sum_x^{a,b,c} (i_{xu} + i_{xl}) + L \frac{d \sum_x^{a,b,c} (i_{xu} + i_{xl})}{dt} \Rightarrow v_{out,HB} = \frac{\sum_x^{a,b,c} (v_{xu} + v_{xl})}{3}. \quad (3)$$

(3) indicates that when an HB-MMC is de-blocked, the generated DC voltage $v_{out,HB}$ is equal to the average of the arm voltages of all three phases. Furthermore, since HB-SMs can only insert positive or zero voltages,

$$\begin{cases} v_{xu} = \max(v_{xu}^*, 0), \\ v_{xl} = \max(v_{xl}^*, 0). \end{cases} \quad (4)$$

Substituting (1) to (4) and (3) gives the relationship between the set-point of the terminal voltage $v_{out,HB}^*$ and the generated DC terminal voltage $v_{out,HB}$ in an HB-MMC. Using (1) to (4), Table 1 provides several pairs of $(v_{out,HB}^*, v_{out,HB})$ and indicates that the minimum voltage $v_{HB,th}$ that an HB-MMC can generate at its DC terminal is $0.622V_m$. This minimum voltage will be used later in Section 5 to evaluate the performance of the restoration algorithm.

Table 1: Several pairs of $(v_{out,HB}^*, v_{out,HB})$

Pair	1	2	3	4	5	6
$(v_{dc}^*, v_{out,HB})$	$(0, 0.622V_m)$	$(0.4V_m, 0.850V_m)$	$(0.8V_m, 1.087V_m)$	$(1.2V_m, 1.354V_m)$	$(1.6V_m, 1.653V_m)$	$(2V_m, 2V_m)$

$$\begin{cases} v_{out} = v_{dc}(t_{db}) + k(t - t_{db}), & t_{db} \leq t \leq t_{db} + \frac{V_{dc} - v_{dc}(t_{db})}{k}, \\ v_{out} = V_{dc}, & t > t_{db} + \frac{V_{dc} - v_{dc}(t_{db})}{k}, \end{cases} \quad (5)$$

As discussed earlier, to have a smooth restoration after the de-blocking of MMCs, the converter terminal voltage v_{out} should be increased gradually from the measured terminal voltage to the nominal DC voltage level. Therefore, in the proposed restoration algorithm, the DC voltage terminal of the converter is controlled according to (5), where $v_{dc}(t_{db})$ is the measured grid voltage when the MMC is de-blocked, and k corresponds to the speed of voltage restoration.

3 TEST SYSTEMS

Three types of four-terminal HVDC grids are tested in this paper: a) a grid with only FB-MMCs called FFFF grid, b) a grid with both HB-MMCs and FB-MMCs called FHFH grid, and c) a grid with only HB-MMCs called HHHH grid as shown in Figure 3. In each grid, MMC1 controls the DC voltage while other MMCs control the active power. The parameters of the test systems are shown in Table 2. Since HB-MMCs cannot interrupt the fault current, an ACCB is inserted between each HB-MMC and the AC grid for fault current interruption.

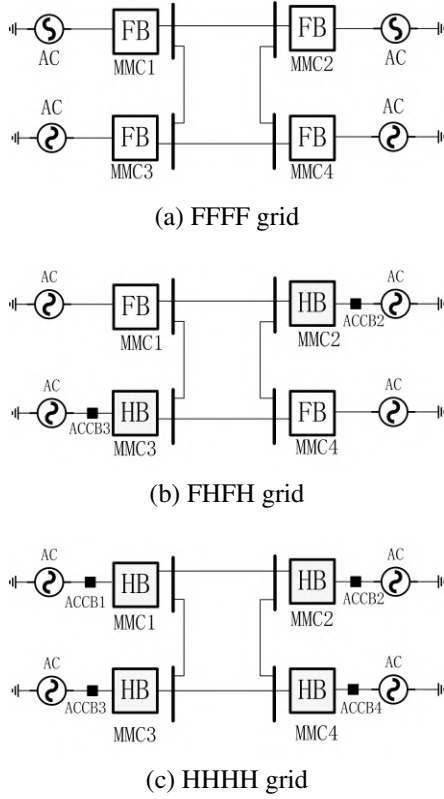


Figure 3: Four-terminal HVDC grids.

4 PROPOSED RESTORATION ALGORITHM

The proposed restoration algorithm has three main steps:

i) Fault isolation investigation: In this step, a voltage-pulse is injected to the grid to determine if the fault has been cleared. To do this, the voltage-controlling MMC (MMC1) is de-blocked for Δt_1 s to inject a voltage pulse V_p to the grid. By comparing the reflected wave at the converter terminal with the pre-fault wave, uncleared faults are detected and the restoration process will be terminated.

ii) Voltage restoration: In this step, MMC1, which control the HVDC grid voltage, is restored. If MMC1 is an FB-MMC, it is de-blocked instantaneously and the grid voltage is gradually increased. If MMC1 is an HB-MMC, it is de-blocked after ACCB1 is closed, which takes about 3 cycles (50 ms). The grid voltage after closing ACCB1 and right before de-blocking MMC1 is given by (6):

$$V_{dc,cls} = \frac{3\sqrt{3}}{\pi} V_m \approx 1.65V_m, \quad (6)$$

where V_m is the peak AC phase voltage. As discussed in Section 2, an HB-MMC can generate a DC terminal voltage larger than $0.622V_m$. Since $1.65V_m$ is larger than $0.622V_m$, the grid voltage is increased from $1.65V_m$ to the nominal value V_{dc} , by gradually increasing the voltage set-point of the voltage-controlling HB-MMC1 according to (5).

iii) Power restoration: In this step, when the DC terminal voltage of MMC n reaches a threshold V_{th} , the converter is restored. If MMC n is an FB-MMC, it is instantaneously de-blocked. If MMC n is an HB-MMC, it is de-blocked after the corresponding ACCB is closed. V_{th} is selected to be three times the magnitude of the voltage pulse V_p to avoid de-blocking of converters, while there are uncleared faults in the grid. In this algorithm, to prevent large inrush currents during restoration, power set-points of the power-controlling MMCs are gradually increased from zero to their nominal values in Δt_2 s.

Table 2: Parameters of the HVDC grid

MMC converter	
Number of SMs per arm	76
Rated SM capacitor voltage	8.5 kV
SM capacitor	3 mF
Arm inductance	50 mH
Control set-points	
Voltage set-point (MMC1)	640 kV
Power set-points (MMC2 & MMC3)	- 900 MW
Power set-point (MMC4)	950 MW
HVDC transmission line	
Rated voltage	640 kV
Rated power	1000 MW
Smoothing inductance	20 mH
Length (all the same)	400 km

5 SIMULATION RESULTS

In the simulation studies of this paper, a pole-to-pole short-circuit fault is applied to the middle of the transmission line connecting MMC1 and MMC2 at $t = 0.01$ s, and the fault impedance is 10Ω . The fault is assumed to be detected in 1 ms. When the fault is detected, MMCs are blocked immediately, and ACCBs are opened in 3 cycles (50 ms). To restore the HVDC grid, first, MMC1, which controls the grid voltage, injects a 200 kV (V_p) pulse into the grid for 0.5 ms. Since the most remote point in the grid is 400 km away from MMC1, it takes less than $400 \text{ km} \times 2/v_{trv} = 2.667$ ms for MMC1 to detect uncleared faults, where $v_{trv} \approx 3 \times 10^8$ m/s is the speed of traveling waves on overhead lines. To ensure that MMC1 is not restored when the fault still exists in the HVDC grid, a safety factor of four is used and MMC1 is fully restored $4 \times 2.667 \approx 10$ ms after injecting the voltage pulse. In the second step, MMC1 will increase the grid voltage with a speed of $k = 32$ kV/ms to the nominal value. $V_{dc,cls}$ in the test systems of this paper is 510 kV. In the third step, $V_{th} = 600$ kV is selected, and power set-points of power-controlling MMCs will increase from zero to their nominal values in $\Delta t_2 = 20$ ms when their MMCs are de-blocked. The performance of the proposed algorithm for the restoration of the three HVDC grids is evaluated in the remaining of this section.

5.1 Restoration of the FFFF grid

In the FFFF grid with four FB-MMCs, all FB-MMCs are blocked at $t = 0.011$ s after the fault occurrence. Since the fault is detected and isolated in 1 ms, fault currents flowing through the four MMCs are not large as shown in Figure 4c. At $t = 0.3$ s, a 200 kV voltage pulse is generated by MMC1 and the reflected waveform at the converter terminal shows that the fault is already cleared and the HVDC grid can be restored. The MMC1 terminal voltage waveform for two scenarios, when the fault is cleared and when the fault still exists, is shown in Figure 4b. MMC1 is de-blocked at $t = 0.31$ s. The other MMCs are de-blocked when the DC voltages at corresponding terminals reach 600 kV. Since the output voltages of the converters are gradually increased from the measured terminal voltages at the de-blocking instant to the nominal voltage, voltage oscillations during the restoration are small, and large inrush currents are prevented as shown in Figure 4. The restoration sequence is provided in Table 3.

The proposed restoration algorithm of this paper is compared against the proposed algorithm of [2] and the comparison is shown in Figure 5, where solid lines show the waveform of the proposed algorithm and dashed lines show the waveform of the algorithm in [2]. Figure 5 shows that the proposed algorithm, compared to the algorithm of [2], restores the HVDC grid faster. However, the algorithm of [2] results in a more smooth rise of the DC voltage as compared to the proposed algorithm of this paper, because fault clearance is not investigated prior to grid restoration in the algorithm of [2]. Even though the injected voltage pulse leads to some voltage oscillations in the proposed algorithm, this voltage pulse enables a safe restoration and attenuates quickly. The proposed algorithm provides faster restoration of the FFFF grid because the algorithm of [2] requires 50 ms to close the ACCBs and energize the grid, which is unnecessary as FB-MMCs do not require ACCBs to interrupt the fault current. Furthermore, in [2] power set-points of power-controlling MMCs are set to zero for 1 s after the MMCs are de-blocked, and are changed to their nominal values at the end of the period. In the proposed algorithm power set-points are increased from zero to their nominal values over a 1 cycle (16.67 ms) period, which significantly accelerates the restoration process and reduces inrush currents.

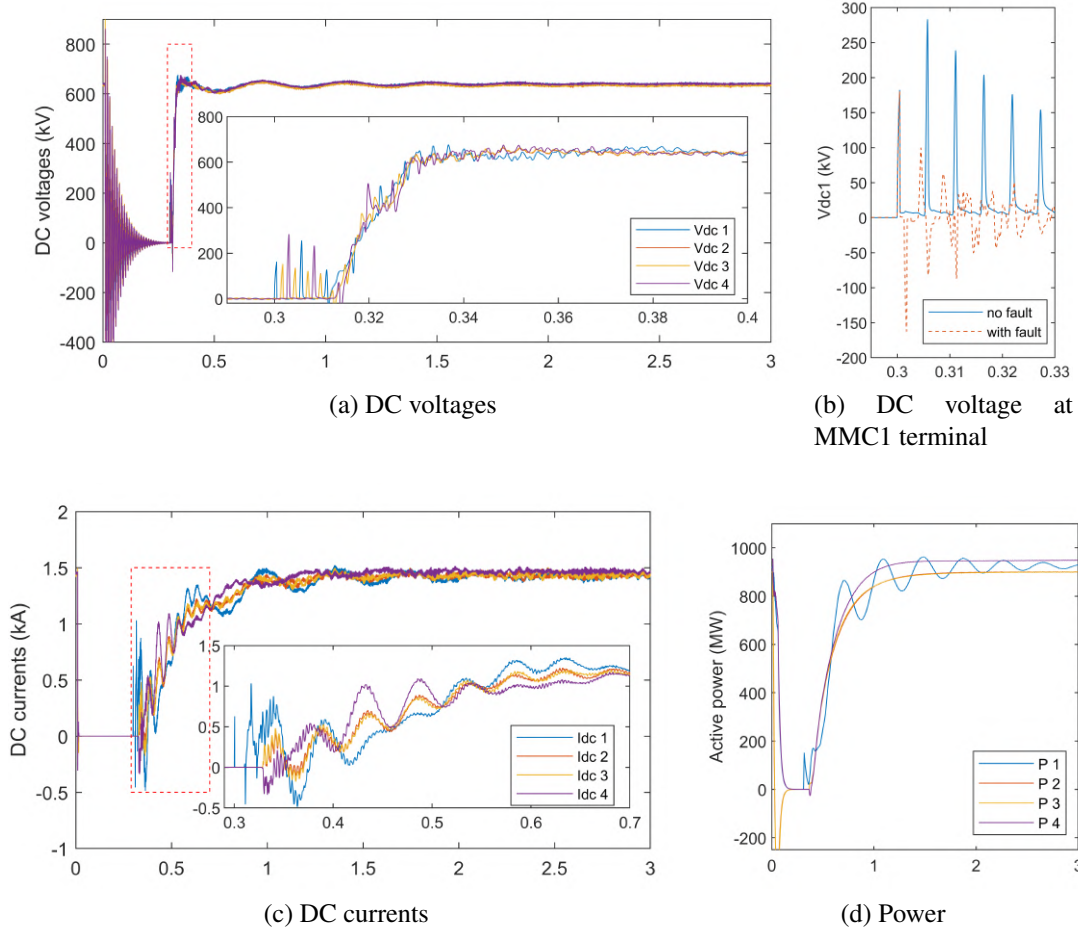


Figure 4: Restoration of the FFFF grid.

5.2 Restoration of the FHFH grid

The fault current in the FHFH grid that contains both FB-MMCs and HB-MMCs is larger than that of the FFFF grid because HB-MMCs cannot interrupt the fault current and rely on ACCBs to clear the fault. Figure 6b shows that after ACCBs trip at $t = 0.061$ s, the fault current gradually decays to zero. Figure 6 shows the DC voltage, current and active power measured at all converter terminals. Figure 6 illustrates that the hybrid HVDC grid is smoothly restored using the proposed restoration algorithm. Figure 6 shows that neither large inrush currents nor large voltage oscillations are caused during the restoration.

Table 3: Restoration sequence of the three HVDC grids

	Proposed algorithm			Algorithm of [2]
	FFFF	FHFH	HHHH	FFFF
Fault identification		0.2		N/A
De-block FB-MMC1 (s)	0.21	0.21	0.27	0.2554
De-block HB-MMC2 (s)	0.2288	0.2888	0.27	0.3096
De-block HB-MMC3 (s)	0.2287	0.2887	0.27	0.2942
De-block FB-MMC4 (s)	0.2291	0.2293	0.27	0.3093
Close ACCB1 (s)	N/A	N/A	0.21	0.2054
Close ACCB2 (s)	N/A	0.2788	0.21	0.2054
Close ACCB3 (s)	N/A	0.2787	0.21	0.2054
Close ACCB4 (s)	N/A	N/A	0.21	0.2054

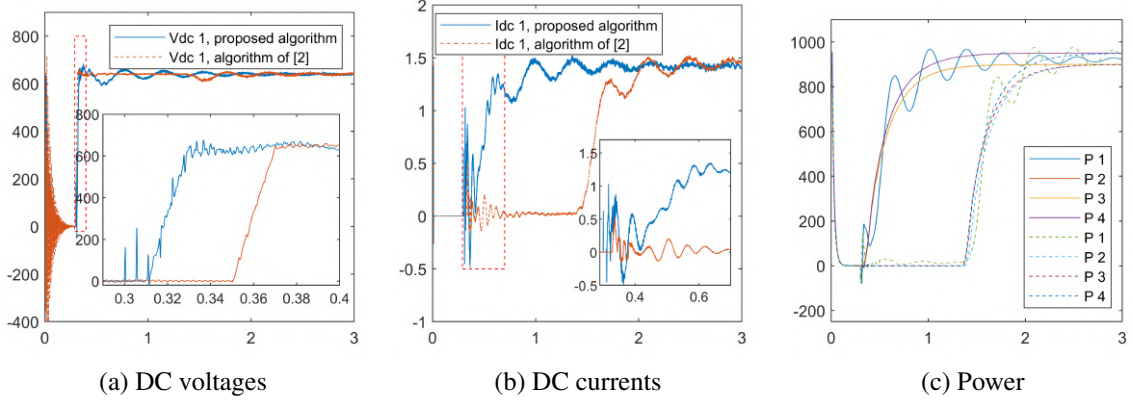


Figure 5: Comparison between the two restoration algorithms applied to the FFFF grid.

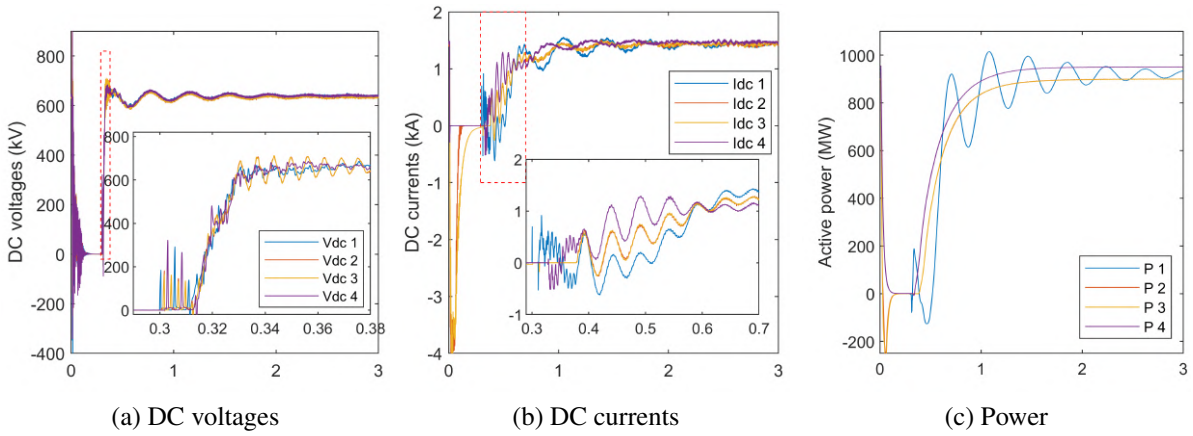


Figure 6: Restoration of the FHHH grid.

5.3 Restoration of the HHHH grid

Figure 7 shows the restoration of the HHHH grid with four HB-MMCs. In this grid, when ACCB1 is closed, a voltage overshoot is caused due to the current flowing through ACCB1. Then, the grid voltage gradually decays to $1.65V_m$. At $t = 0.36$ s, HB-MMCs are de-blocked and the grid voltage is restored to the nominal value.

6 CONCLUSION

This paper proposes a restoration algorithm for HVDC grids with any combination of converters with and without fault blocking capability. In this restoration algorithm, first, traveling waves resulted from a voltage-pulse injection from one of the converters to the grid is used to identify any uncleared faults. If no existing fault is detected, the converter controlling the grid voltage is first restored to establish the grid voltage, and consecutively converters that control the grid power are restored. The proposed restoration algorithm specifies the proper sequence for the restoration of all different types of converters forming the HVDC grid. The restoration of three HVDC grids, which include FB-MMCs, HB-MMCs, or a combination of FB-MMCs and HB-MMCs, is studied in this paper. To prevent large voltage oscillations and to limit inrush currents, the proposed restoration algorithm increases the terminal voltages of the converters from the measured values to the nominal value and gradually energizes the grid. Also, the power set-points of power-controlling MMCs are increased from zero to their set-point values over one cycle to prevent large inrush currents. Simulation results show that the proposed restoration

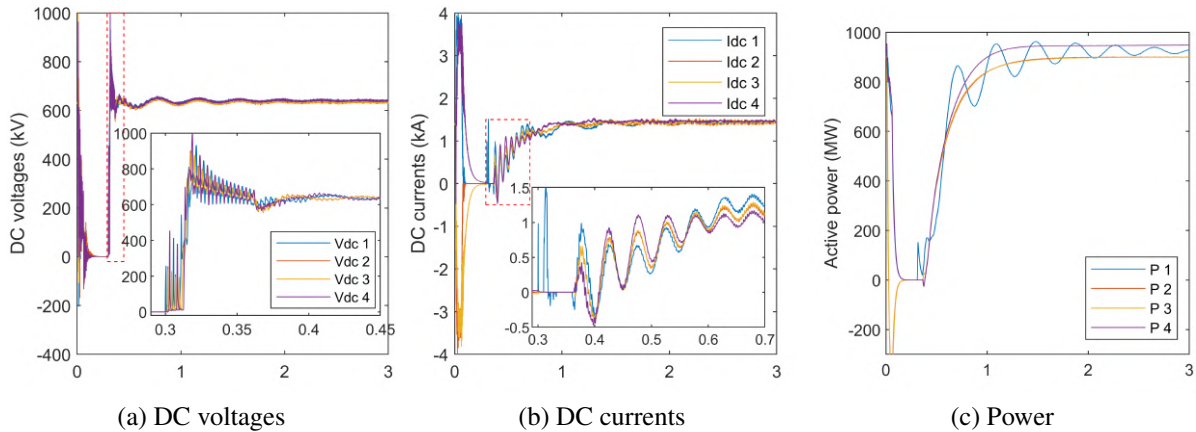


Figure 7: Restoration of the HHHH grid.

algorithm can restore different types of grids including hybrid HVDC systems in less than 40 ms, with limited inrush currents and low voltage oscillations.

REFERENCES

- [1] Bin Li, Jiawei He, Ye Li, and Weijie Wen. A Novel DCCB Reclosing Strategy for the Flexible HVDC Grid. *IEEE Transactions on Power Delivery*, 35(1):244–257, feb 2020.
- [2] E. Kontos, R. Teixeira Pinto, and P. Bauer. Providing dc fault ride-through capability to H-bridge MMC-based HVDC networks. In *9th International Conference on Power Electronics - ECCE Asia: "Green World with Power Electronics", ICPE 2015-ECCE Asia*, pages 1542–1551. Institute of Electrical and Electronics Engineers Inc., jul 2015.
- [3] Tianshu Bi, Shuai Wang, and Ke Jia. Single pole-to-ground fault location method for MMC-HVDC system using active pulse. *IET Generation, Transmission and Distribution*, 12(2):272–278, jan 2018.
- [4] Willem Leterme, Sahar Pirooz Azad, and Dirk Van Hertem. HVDC grid protection algorithm design in phase and modal domains. *IET Renewable Power Generation*, 12(13):1538–1546, oct 2018.
- [5] Guobing Song, Ting Wang, and Kazmi S.T. Hussain. DC Line Fault Identification Based on Pulse Injection from Hybrid HVDC Breaker. *IEEE Transactions on Power Delivery*, 34(1):271–280, feb 2019.
- [6] Shenghui Cui and Seung Ki Sul. A Comprehensive DC Short-Circuit Fault Ride Through Strategy of Hybrid Modular Multilevel Converters (MMCs) for Overhead Line Transmission. *IEEE Transactions on Power Electronics*, 31(11):7780–7796, 2016.
- [7] Song Tang, Guanlong Jia, Chenghao Zhang, and Min Chen. A modified DC fault protection scheme for multi-terminal HVDC grid based on fault current limiters. In *2019 4th IEEE Workshop on the Electronic Grid, eGRID 2019*. Institute of Electrical and Electronics Engineers Inc., nov 2019.
- [8] Willem Leterme, Jef Beerten, and Dirk Van Hertem. Nonunit protection of HVDC grids with inductive DC cable termination. *IEEE Transactions on Power Delivery*, 31(2):820–828, apr 2016.
- [9] Arjun Visakh and R. M. Shereef. Protection of HVDC Grids Against Temporary and Permanent Faults. In *2018 International Conference on Control, Power, Communication and Computing Technologies, ICCPCCT 2018*, pages 239–244. Institute of Electrical and Electronics Engineers Inc., dec 2018.
- [10] Mohammad Farshad. Ultra-high-speed non-unit non-differential protection scheme for buses of MMC-HVDC grids. *IET Renewable Power Generation*, 14(9):1541–1549, jul 2020.
- [11] Rui Dantas, Jun Liang, Carlos Ernesto Ugalde-Loo, Andrzej Adamczyk, Carl Barker, and Robert Whitehouse. Progressive Fault Isolation and Grid Restoration Strategy for MTDC Networks. *IEEE Transactions on Power Delivery*, 33(2):909–918, 2018.